proceedings

MDPI

Type of the Paper (Proceeding Paper, Abstract, Editorial, etc.)

Development of far-Infrared detectors for nondestructive inspection of infrastructure buildings †

Kazuma Iwasaki [1,*], Seishi Abe [2] and Tadao Tanabe [3]

[1] Department of Functional Control Systems, Shibaura Institute of Technology; md22009@shibaura-it.ac.jp
[2] Research Institute for Electromagnetic Materials; abe@denjiken.ne.jp
[3] Department of Design Engineering, Shibaura Institute of Technology; tanabet@shibaura-it.ac.jp
* Correspondence: md22009@shibaura-it.ac.jp; Tel.:03-5859-8828
† Kobe, Japan, September 15 to 19, 2025

Abstract: In nondestructive evaluation of concrete structures, the far-infrared region, including terahertz waves, which can penetrate concrete and measure the amount of corrosion in the internal steel, has attracted much attention. Magnetite has the potential to be used as a far-infrared detection device that meets the requirements for nondestructive evaluation devices, such as room temperature operation and portability, while also having a low environmental impact. In this study, the sensitivity of magnetite thin films with different concentrations of Pt to electromagnetic waves at a wavelength of 10.6 ㎛ was evaluated and compared: nanocomposite with Pt nanocrystals despersed in magnetite thin films were prepared by radio-frequency sputtering, electrodes were prepared by a photoresist process, and the resistance variation was recorded after irradiation with 10.6 ㎛ pulse electromagnetic waves. As a result, it was experimentally confirmed that the peak of response was the maximum at the amount of Pt added where the electrical resistivity reached 12,000 μΩcm, and the S/N ratio was the maximum at the amount of Pt added where the electrical resistivity reached 14,000 μΩcm. This indicates that Pt-doped magnetite with a Pt content of 14,000 μΩcm electrical resistivity is suitable as a far-infrared detector element material.

Keywords: Magnetite；Integration; Photodetector; Terahertz wave; Nondestructive evaluation

1. Introduction

Electromagnetic waves in the far-infrared region, including terahertz waves, can penetrate concrete and measure reflected waves from internal reinforcing steel. In addition, the frequency range of this region is less harmful to the human body because the energy is close to room temperature [1]. Because of these characteristics, nondestructive evaluation of concrete structures using electromagnetic waves in the far-infrared region, including terahertz waves, has attracted much attention. However, the challenge for practical use is that few detectors have practical features such as stable operation in environments above room temperature, high sensitivity to detect faint scattered light, and portability to work in high places. Although the development of detector arrays in the terahertz wave range has also been studied, they have not yet been implemented in society [2]. Table 1 ranks the major single element infrared detectors from 1 to 5 in terms of

Academic Editor: Firstname Lastname

Published: date

Citation: To be added by editorial staff during production.

nondestructive evaluation , including device size, device weight, operating environment, power supply size, detection sensitivity, and broadband response. The closer the level is to 1, the more suitable it is for nondestructive evaluation, and the closer to 5, the less suitable. There is a trade-off between sensitivity and items related to portability, including size, weight, and operating environment; the higher the sensitivity, the less portable the device. Currently, the detectors in practical use that have performance similar to the practical functions described above are narrow bandgap semiconductor detectors. These semiconductors use rare and highly toxic materials to the human body, such as mercury (Hg) and cadmium (Cd). The future widespread use of nondestructive evaluation applications in the far-infrared region, including terahertz waves, will require detectors made of materials that are practical, yet safe and have a low environmental impact. Therefore, we focused on magnetite (Fe_3O_4), which has a band gap of 0.1 eV [3], and evaluated the photoresponse of magnetite. Magnetite is a type of iron oxide, which is abundant in the earth and can be reused by refining, thus having a low environmental impact. Furthermore, it is highly biodegradable and has low toxicity to the human body [4]. Another advantage of magnetite, an iron oxide, is that the band gap can be tuned. It has been reported that when Zn is added to α-Fe2O3, which is an iron oxide like magnetite, the band gap decreases at Zn concentrations up to 4% [5], and by changing the structure by introducing defects, etc., a response in the low-frequency range can be expected.In our previous study, magnetite thin films with an area of approximately 10 x 10 mm^2 deposited by radio-frequency (RF)sputtering were irradiated with pulsed electromagnetic waves of 10.6 μm wavelength (=28 THz = 0.12 eV) in a room temperature environment to evaliate their response to electromagnetic waves [6]. This result indicates the applicability of magnetite as a detector with portability and room temperature operation. The addition of 9.4 at.% platinum (Pt) reduced the resistance by two orders of magnitude compared to no addition, but there was no significant difference in sensitivity [6]. Since the work function of Pt is larger than the electron affinity of magnetite [7], Pt nanocrystals dispersed in a magnetite film are expected to capture the electrons generated in magnetite before their lifetime expires. Therefore, the sensitivity of the detector is expected to be improved compared to magnetite without Pt, but in the previous study, the relatively large number of Pt nanocrystals reduced the volume fraction of magnetite in the thin film, which did not contribute to improved sensitivity [6]. In other words, detector sensitivity is a trade-off between the volume ratio of Pt nanocrystals and magnetite, and the optimal Pt addition concentration needs to be clarified. In this study, magnetite thin films with different Pt adding concentrations were irradiated with pulsed electromagnetic waves, and the sensitivity was evaluated.

Table 1. Ranks of major infrared detectors in nondestructive detection

Detector	Size	Weight	Environment	Power supply	Sensitivity	Broadband	Average
HgCdTe(MCT)	2	2	5	2	2	4	2.8
InSb, PbSe	2	2	2	1	3	5	2.5
Si bolometer	5	5	5	5	1	1	3.7
DTGS	2	2	3	2	4	2	2.5
Golay cell	3	3	4	5	3	3	3.5
Photoconductive antenna	5	5	5	2	3	2	3.7
Schottky barrier diode	1	1	1	2	3	3	1.8

2. Methods

Nanocomposite thin films with Pt nanocrystals despersed in magnetite was deposited on a glass substrate of approximately 10 x 10 mm^2 by RF sputtering, and the concentration of Pt addition was controlled by the number of Pt chips attached to the magnetite target. Table 2 shows the Pt concentration, electrical resistivity, and number of Pt chips used for each sample. The platinum concentration was measured by Energy Dispersive X-ray Spectroscopy (EDS). Although the platinum addition concentrations of samples #4 and #5 are the same, the electrical resistivity (Four-terminal measurement) and the number of platinum chips are different, so the concentrations are considered to vary below the resolution of EDS. Electrodes were prepared by photolithography using a maskless exposure system (DL-1000GS/SS, NanoSystem). Resist (OFPR-800, Tokyo Ohka Kogyo Co., Ltd.) was applied to the substrate and exposed with g-line (wavelength 436 nm). The electrode was made of platinum and prepared by RF sputtering: RF power was 400 W, sputtered for 6 min, and an electrode of approximately 120 nm was deposited. The irradiated electromagnetic wave was a CO_2 laser with a wavelength of 10.6 μm and a power density of 0.04 W/cm^2, adjusted to a pulsed wave by a chopper. Pulse widths were adjusted to 0.5 s, 0.25 s, 0.1 s, 0.0625 s, and 0.05 s. Measurements were made by probing the padded portion of the electrode and measuring the resistance. Differentiated time waveforms of resistance values were used in the analysis.

Table 2. Pt concentration, electrical resistivity and number of Pt chips in Pt-added Fe_3O_4 samples

Sample number	Pt concentration (at.%)	Electrical resistivity ($\mu\Omega$cm)	Pt chips
#1	6.9	4.1×10^3	8
#2	6.3	4.6×10^3	6
#3	3.8	6.6×10^3	4
#4	1.6	1.2×10^4	2
#5	1.6	1.4×10^4	1

3. Results

The average peak intensity was calculated based on 10 response peaks. Figure 1(a) plots the electrical resistivity on the horizontal axis and the average peak intensity on the vertical axis. The response peaks of samples #4 and #5 with similar platinum addition concentrations tended to be larger in sample #4. The signal-to-noise ratio was calculated by dividing this peak intensity by the rms value of noise during 30 s. Figure 1(b) plots electrical resistivity on the horizontal axis and signal-to-noise ratio on the vertical axis; sample #5 has the highest signal-to-noise ratio, and this result experimentally confirmed that the highest sensitivity is obtained at a platinum concentration of 1.6 at.%, which results in electrical resistivity near 1.4×10^4 μΩcm. Sample #4 has the highest peak intensity, but the signal-to-noise ratio is low because the noise level is also large,

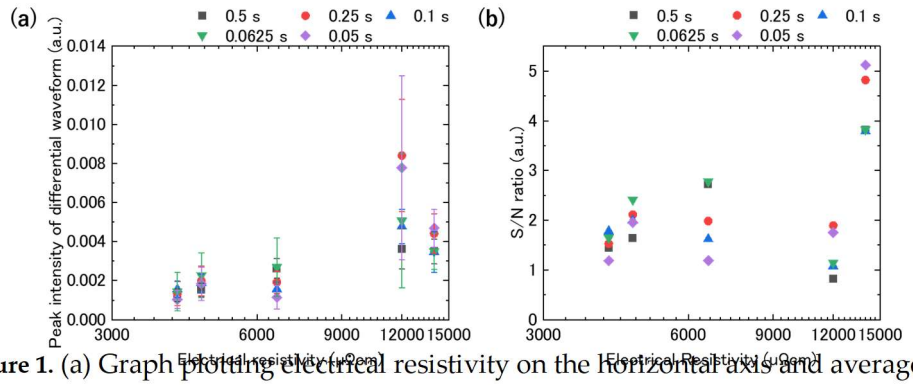

Figure 1. (a) Graph plotting electrical resistivity on the horizontal axis and average peak intensity on the vertical axis. (b) Graph plotting electrical resistivity on the horizontal axis and S/N ratio on the vertical axis.

confirming that the photoresponses of samples #4 and #5 with different Pt-doping concentrations differ greatly below the resolution of EDS.The change in responsivity with pulse width of the electromagnetic wave was confirmed. This result indicate that sample #5 is suitable as a far-infrared detector element material.

4. Conclusions

In this study, we searched for the optimal amount of Pt added to magnetite, which is expected to have potential application as a detector with low environmental impact, portability, and room temperature operation, in order to improve sensitivity. When irradiated with a pulse of 10.6 μm wavelength, the response peaked at a peak of 1.6 at.% Pt at a resistivity of 12,000 μΩcm, which is the maximum for sample #4. However, sample #4 had a large noise level, and the sensitivity as a signal-to-noise ratio was experimentally confirmed to be maximum in sample #5 with a Pt content of 1.6 at.%, where the electrical resistivity was 14,000 μΩcm. This indicates that nanocomposite thin films with Pt nanocrystals despersed in magnetite that results in an electrical resistivity of 14,000 μΩcm is suitable for far-infrared detectors.

Author Contributions: Conceptualization, S.A. and T.T.; Formal analysis, K.I., S.A. and T.T.; investigation, K.I..; resources, S.A.; writing—original draft preparation, K.I. All authors have read and agreed to the published version of the manuscript.

Funding: This research was funded by Japan Science and Technology Agency, grant number JPMJSP2168.

Informed Consent Statement: Not applicable

Data Availability Statement: The data that support the finding of this study are available from the corresponding author upon reasonable request.

Conflicts of Interest: The funders had no role in the design of the study; in the collection, analyses, or interpretation of data; in the writing of the manuscript; or in the decision to publish the results.

References

1. Yu J.; Liu X.; Manago G.; Tadao T.; Osanai S.; and Okubo K. New Terahertz Wave Sorting Technology to Improve Plastic Containers and Packaging Waste Recycling in Japan. *Recycling*, **2022**, 7, 5, 66. [CrossRef]
2. Li K.; Araki T.; Utaki R.; Tokumoto Y.; Sun M.;Yasui S.; Kurihira N.; Kasai Y.; Suzuki D.; Marteijn R.; Toonder J. M. J. D.; Sekitani T.; and Kawano Y. Stretchable broadband photo-sensor sheets for nonsampling, source-free, and label-free chemical monitoring by simple deformable wrapping. *Science Advances* **2022**, 8, 19, eabm4349. [CrossRef]
3. Merchant P.; Collins R.; Kershaw R.; Dwight K.; and Wold A. The electrical, optical and photoconducting properties of $Fe_{2-x}Cr_xO_3$ ($0 \leqslant x \leqslant 0.47$). *J. Solid State Chem*. **1979**, 27, 307-315. [CrossRef]
4. Klekotka U.; Zambrzycka-Szelewa E.; SatułaD.; and Kalska-Szostko B. Stability Studies of Magnetite Nanoparticles in Environmental Solutions. *Materials* **2021**, 14, 17, 5069. [CrossRef]
5. Suman ; Chahal S.; Kumar A.; and Kumar P. Zn Doped α-Fe_2O_3: An Efficient Material for UV Driven Photocatalysis and Electrical Conductivity. *Crystals* **2020**, 10, 4, 273.
6. Iwasaki K.; Abe S.; Tanabe T. Mid-infrared detection device using magnetite substrates deposited by radio frequency sputtering method. *AIP Advances.* **2025**, 15, 015127. [CrossRef]
7. Abe S. Nanocomposite thin films containing Pt nanoparticles dispersed in an α-Fe2O3 matrix by RF sputtering. AIP Advances. **2024**, *14*, 025348. [CrossRef]